Sensors and Materials, Vol. 34, No. 7 (2022) 2687–2707
MYU Tokyo

S & M 2999

Multi-agent Simulation Scenarios for Evacuation within Children's Facilities through Merged Machine Learning Techniques and Multilayer Vulnerability Analysis

Ever Enrique Castillo Osorio, Min Song Seo, and Hwan Hee Yoo*

Department of Urban Engineering, Gyeongsang National University,
501, Jinju daero, Jinju, Gyeongsangnam-do 660701, Korea

(Received Mach 23, 2022; accepted June 13, 2022; online published June 27, 2022)

Keywords: multilayer analysis, machine learning, multi-agent system, pathfinding, collision avoidance

Evacuation plans in buildings where people perform activities must be clearly defined. Children's facilities are a special case in which indoor navigation must be traced by safe routes. However, usually, the routes follow the shortest path. We propose the calculation of safer evacuation routes inside a multi-agent kindergarten environment using the angle propagation theta*-multilayer vulnerability analysis (AP-Theta*-MVA) algorithm, a novel variant of the angle propagation theta* (AP-Theta*) pathfinding technique. In this variant, we perform the multilayer vulnerability analysis (MVA) of geometric objects based on international standards to obtain importance indexes (*Sn*). In addition, we include rules of the reciprocal *n*-body collision avoidance approach (ORCA) and the conditioning variables of the location of the hazard, the number of people, and their speed of movement and reaction ability. We apply the algorithm in different scenarios of evacuation due to fire smoke propagation within a children's facility. Our results show that for each scenario, AP-Theta*-MVA provides orders through signals obtained by supervised learning to the multi-agent system to react and move away from dangerous areas. Thus, we achieve safer evacuation patterns and routes for a multi-agent system. This demonstrates the suitability of the AP-Theta*-MVA algorithm, which is influenced by the MVA, for children's facilities when it is performed in a multi-agent system, enabling the calculation of safe and feasible evacuation routes with realistic times to improve evacuation plans.

1. Introduction

When an emergency situation arises, it is important to clearly know the predefined safe evacuation routes of buildings. One of the most critical cases is evacuation within children's facilities because of the high vulnerability of children.[1] Therefore, in facilities designed for children, priority must be given to evacuation routes that ensure their safe movement and prevention from harm.

Standards have been developed worldwide for the design and construction of safe children's facilities.[2–5] In addition, research applying various pathfinding algorithms has been performed to calculate and simulate evacuation routes from inside buildings.[6–8] One of the most basic but

*Corresponding author (ERI): e-mail: hhyoo@gnu.ac.kr
https://doi.org/10.18494/SAM3902

ISSN 0914-4935
https://myukk.org/

effective algorithms for pathfinding was proposed by Dijkstra, in which, through pairs of points with shorter distances, a route is created to reach a final node.[9] On this basis, Hart *et al.* proposed the A-star (A*) algorithm, which incorporates heuristic data in decision making for route selection.[10] Daniel *et al.* compared the use of various pathfinding algorithms, such as Field D*, A*, Theta*, and AP-Theta*, showing that the latter finds shorter routes and simulates more realistic conditions of movement than the other techniques.[11] Naderpour also verified the usefulness of route search algorithms, finding that the AP-Theta* model was the most advantageous for realistically simulating human movement behavior.[12] Simulations of evacuation activities using different collision avoidance techniques for multi-agent systems have also been performed.[13–16] However, the main factor that is always prioritized is the evacuation time, forcing the tracing of shorter paths to the exits. These short paths do not consider other criteria, such as the vulnerability of the elements that are part of the suggested routes. Therefore, these paths may differ from those in a real emergency evacuation event in which different physical and human factors influence the choice of paths followed by people.

In this study, we propose a novel angle propagation theta*-multilayer vulnerability analysis (AP-Theta*-MVA) algorithm that, through merged machine learning techniques, prioritizes levels of vulnerability and physical and human conditioning variables for the calculation of safe and feasible evacuation routes within children's facilities. The AP-Theta*-MVA algorithm is a variant of the angle propagation theta* (AP-theta*) pathfinding algorithm. Moreover, it works under the supervised learning technique that, through signals, provides instructions to the agents to react and move towards a nearby exit. The algorithm is applied to different simulation scenarios of multi-agent systems influenced by importance indexes (*Sn*) obtained from the multilayer vulnerability analysis (MVA) of the facilities. The structural and non-structural elements of the facilities and their attributes such as the distribution, location, materials, design, and conditions are obtained from spatial data layers arranged by types of vulnerability and migrated from a building information modeling (BIM) as simplified vectors.[17] Subsequently, the multilayer vulnerability conditions for children's facilities are classified under international standards and analyzed in a suitability table. The results of the MVA are validated by the analytical hierarchy process (AHP).[18–20] *Sn* are calculated and added as input heuristic data in the AP-Theta*-MVA algorithm. AP-Theta*-MVA performs indoor navigation considering conditioning variables such as the location of the hazard, the number of people, and their speed of movement and reaction ability as the input for simulation scenarios. In addition, the algorithm includes rules of the reciprocal n-body collision avoidance approach (ORCA). This approach avoids collisions between agents by reducing their speeds equally when the distances between them are less than a specified collision risk buffer.[21] All these conditions are interpreted by AP-Theta*-MVA, which provides instructions to agents for their movement and calculates safer evacuation times and routes. The multi-agent system for different simulation scenarios is tested by NetLogo software. The methodology is applied in a case study in which smoke spreads from a fire inside children's facilities, with the dispersion of the smoke based on the automatic mesh generation (MG) algorithm.[22,23] The AP-Theta*-MVA algorithm simulates scenarios and prioritizes the most feasible and safest routes for evacuation plans and for the design of construction projects with safety standards.

2. Methodology

The geometric objects of children's facilities are designed in a BIM and linked to vulnerability data taken from international standards. Simplified vector multilayers are generated. Their vulnerability criteria are classified through a suitability model and comparison matrices. Weights are assigned to the layers, and the results are validated using the AHP to obtain *Sn*. These indexes are used as heuristic data together with other conditioning variables, such as the location of the hazard, the number of people, and their speed of movement and reaction ability, and are input in the AP-Theta*-MVA algorithm. This algorithm is applied in a multi-agent system environment that also includes rules of AP-Theta* pathfinding and ORCA collision avoidance as supervised machine learning techniques. The simulations are performed for different evacuation scenarios in which fire smoke spreads inside children's facilities to obtain feasible evacuation routes. Furthermore, the evacuation times, the percentage of people who escape to safe areas, and the percentage of people who are trapped when surrounded by fire smoke are also calculated for each simulation scenario to validate the feasibility of the routes proposed in the multi-agent system. The methodological process is shown in Fig. 1.

2.1 Spatial data layer processing

Through the use of a BIM, the complexity of indoor spatial objects in children's facilities is arranged. The BIM allows the data of the elements to be classified into two groups: geometric and tabular. The geometric data comprises the geospatial location of the set of vertices that are part of each element to guarantee their spatial distribution and the physical connection between them. Tabular data includes the architectural, mechanical, and material characteristics, as well

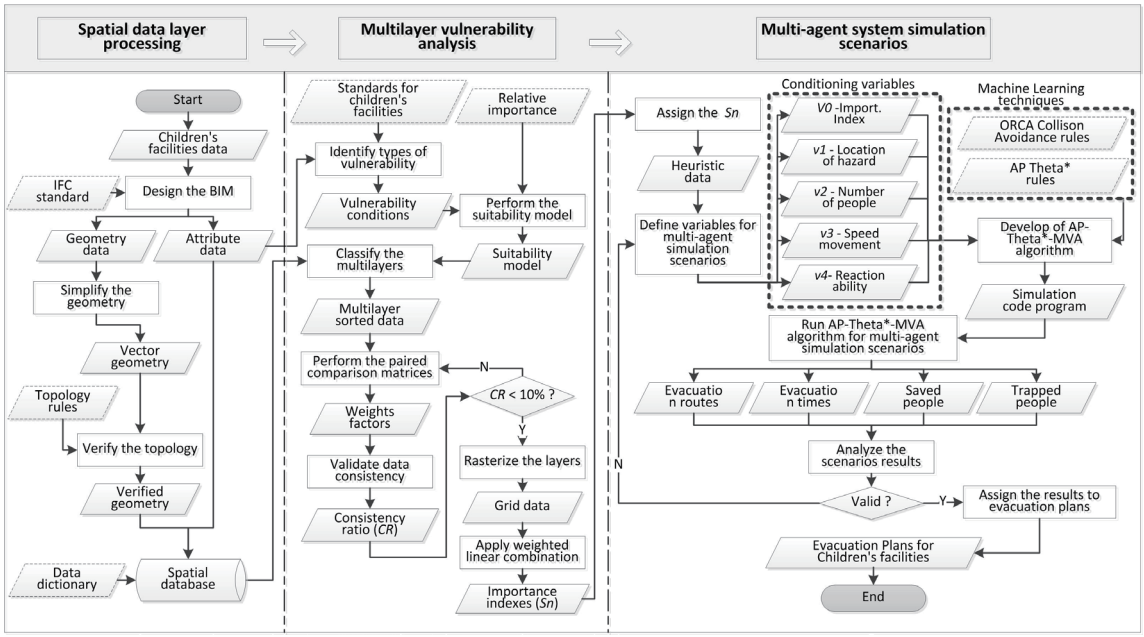

Fig. 1. Methodology process flowchart.

as the vulnerability conditions of the structural and non-structural objects of the children's facilities and the relational information among them.[24] The Industry Foundation Classes (IFC) standards shown in Table 1 are used for the coding and organization of BIM data.

This study considers not only the structure of the building in various IFC standards, but also the non-structural elements such as fixed furniture (tables, desks, chairs, cabinets, etc.), through the IFC Furniture standard. This standard together with IFC Column and IFC Wall are considered as obstacles in the model. Likewise, the doors stored in IFC Door are a group excluded in the simulation, since it is assumed that no interior doors block the transit of people. The geometric data is reconstructed in a simplified geometry based on polygons. Topological rules are applied to the polygons to avoid overlap between neighboring objects. Simplified data objects are stored in a spatial database. The logical model of the database structure, which saves the results of applying the IFC standards to simplified objects, is shown in Fig. 2. Likewise, the descriptions of the database tables are given in Table 2.

Table 1
IFC standards.

Structural elements				
IFC classes	IFC geometry code	Object category	Element name	Example
IFC wall	IfcSurface	Space boundary	Wall	Wall, partition
IFC column	IfcSurface	Space boundary	Column	Column
Non-structural elements				
IFC classes	IFC geometry code	Object category	Element name	Example
IFC room	IfcSurface	Space	Room	Classroom, lab, office
IFC space	IfcSurface	Space	Space	Floor
IFC door	IfcPolyline	Horizontal portal	Door	Door
IFC furniture	IfcSurface	Furnishings	Furniture	Desk, table
IFC electric appliance	IfcSurface	Flow terminal	Electric appliance	Power box, IT rack

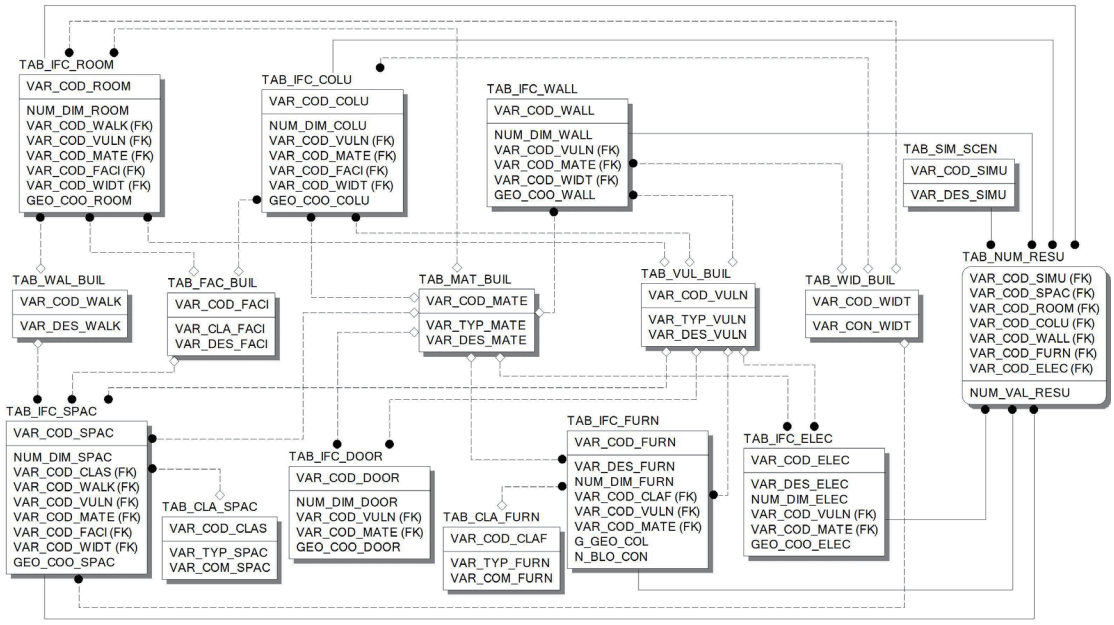

Fig. 2. Spatial database model.

Table 2
Descriptions of database tables.

Spatial tables	
Standard name	Description
Structural elements	
TAB_IFC_WALL	Wall
TAB_IFC_COLU	Column
Non-structural elements	
TAB_IFC_ROOM	Room
TAB_IFC_SPAC	Space
TAB_IFC_DOOR	Door
TAB_IFC_FURN	Furniture
TAB_IFC_ELEC	Electric appliance

Non-spatial tables	
Standard name	Description
TAB_VUL_BUIL	Vulnerability
TAB_MAT_BUIL	Material
TAB_FAC_BUIL	Facility
TAB_WAL_BUIL	Walkability
TAB_WID_BUIL	Width
TAB_CLA_FURN	Classification of furniture
TAB_CLA_SPAC	Classification of spaces
TAB_SIM_SCEN	Simulation scenario type
TAB_NUM_RESU	Numerical results

2.2 Multilayer vulnerability analysis

From the spatial database, the features related to vulnerability conditions are selected. They are classified under the specific standards of the Design Guide for Improving School Safety in Earthquakes, Floods, and High Winds of the Federal Emergency Management Agency (FEMA) of the United States.[2] The vulnerability layers are selected in consideration of the protection methods of the building system in children's facilities to minimize the impact of multiple hazards such as earthquakes, floods, winds, security/blasts, and fire. In addition, the width condition of the areas, proposed by the Americans with Disabilities Act (ADA) of the United States, is also considered.[25] This is included since in a multi-agent system, the transit of people is expected to be both sequential and parallel. The list of vulnerability layers is shown in Fig. 3

The AHP method is used to analyze the vulnerability conditions in all the layers, compare them with each other through paired matrices, classify them according to their priority, and validate the coherence of this prioritization for each group.[26] The flowchart in Fig. 4 details the

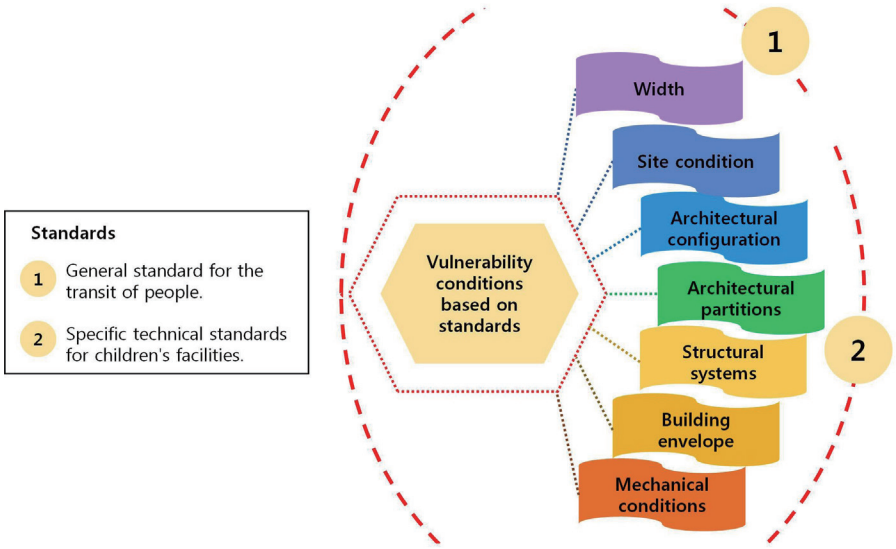

Fig. 3. (Color online) Classification of vulnerability layers.

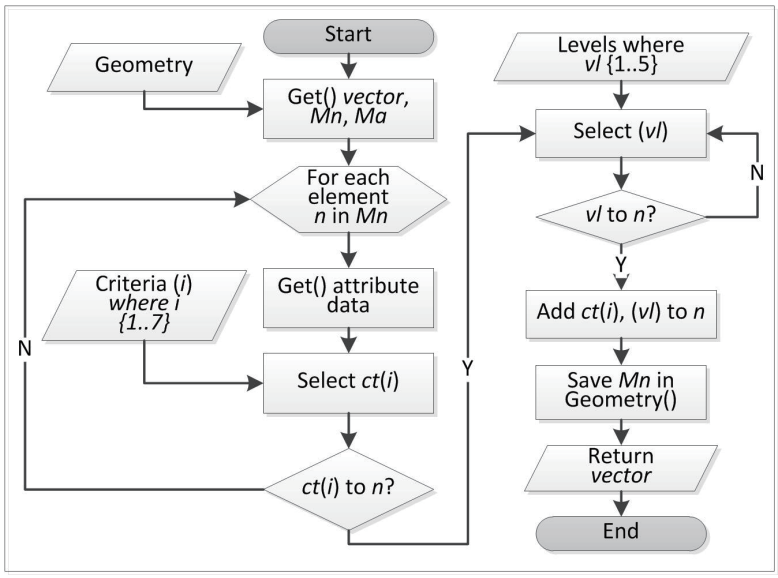

Fig. 4. Flowchart of the level classification based on a suitability model.

pseudo-code of the level classification based on a suitability model, where *vector* is the selected feature layer, *n* is the selected element, *Mn* and *Ma* are the matrices of the geometric and attribute data, respectively, *ct*(*i*) is the type of criteria, and *vl* is the vulnerability level. The conditions are prioritized according to the vulnerability level related to the occurrence of the hazard in the multi-agent environment.

The range of vulnerability levels is from 1 to 5, with a value of 1 given to elements with the least vulnerability and guaranteeing the safest movement within children's facilities in the case of a disaster. On the other hand, the elements with the greatest vulnerability in the case of a disaster and most unsafe for movement in children's facilities are given a value of 5. The levels are applied for each vector within each vulnerability layer. These classifications are assigned on the basis of the hazard being analyzed, since the response, behavior, and levels of vulnerability of the elements are different for each hazard. Subsequently, the vulnerability layers are compared through the use of paired matrices to determine their level of influence on each other. Through the AHP method, weights interpreted as *Sn* are assigned for each vulnerability layer. The consistency of the model is evaluated by obtaining the consistency ratio (*CR*), which must have a value of less than 10% to guarantee consistency.[19] Finally, through the weighted linear combination (WLC) method, the vulnerability layers are rasterized to save their *Sn* information.[20]

2.3 Multi-agent system simulation scenarios

The AP-Theta*-MVA algorithm performs the movement of agents inside children's facilities. It works under supervised learning techniques based on the rules of AP-Theta* pathfinding and the ORCA collision avoidance method. In addition, the algorithm considers *Sn* as variable *v*0 and includes other conditioning variables that parameterize the initial conditions, producing different

simulation scenarios that allow a better analysis of evacuation proposals. These conditioning variables are the location of the hazard ($v1$), the number of people ($v2$), and their speed of movement ($v3$) and reaction ability ($v4$). The AP-Theta*-MVA algorithm data flow scheme is shown in Fig. 5.

The supervised learning techniques allow the AP-Theta*-MVA algorithm to assign functions to the agents to ensure their movement through safe areas with the aim of reaching the target node (N_t) and avoiding the collision between them or with other fixed obstacles. Specifically AP-Theta* pathfinding is a variant of the A* algorithm. The main advantage of the AP-Theta* algorithm is that it reads the initial node N_{i1} of the agent and evaluates the heuristic function of the final node N_{f1} to which this agent can potentially be displaced within a section in order to reach N_t.[27] The potential final nodes are distributed in the section and located within a range in the line of sight (LOS) from the initial node N_{i1}. The amplitude of the LOS is defined by angles θ_1 and θ_2, which are limited by the obstacles located in the surroundings. The angle range in the AP-Theta* algorithm applied to every section is described in Eq. (1), where $\theta = \theta_1 + \theta_2$; N_i = initial node; N_f = final node; e_x = edge of angle θ; x = value {1,2}; i = value {1…n}.

$$\theta_x\left(N_f, N_i, e_x\right) \in \left[-180°, 180°\right] \tag{1}$$

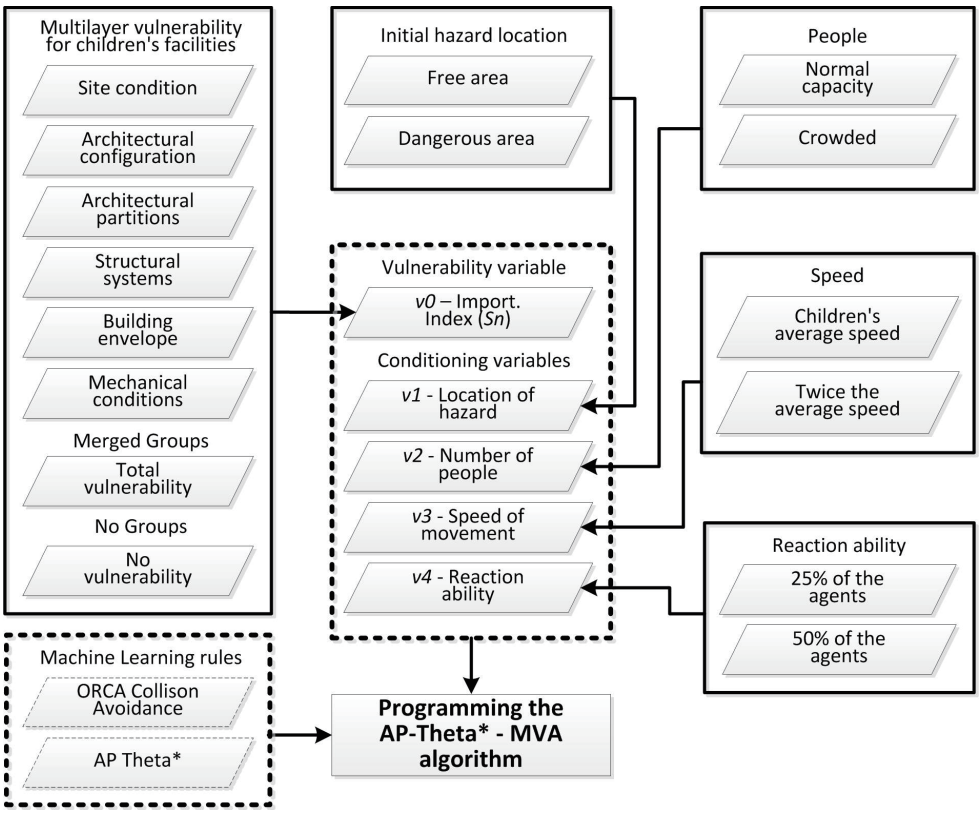

Fig. 5. AP-Theta*-MVA algorithm data flow scheme.

The AP-Theta* algorithm evaluates and selects N_{f1} for the displacement of an agent in the first section. When an agent is placed there, it becomes a new initial node N_{i2} and the process is repeated until the end node N_{fn} of the last section coincides with N_t. An example of the displacement between the nodes under AP-Theta* is shown in Fig. 6. The agent must move from N_{i1} [A1] to N_t [D3]. In Fig. 6(a), the LOS allows the agent located in [A1] to visualize the surrounding nodes [A2], [A3], [B1], [B2], [B3], [C1], [C2], [D1], and [D2], but there is no direct LOS to node [D3] due to obstacles in the area. The algorithm selects node [C2] as the temporary N_f because it is closest to N_t. In Fig. 6(b), node [C2] becomes the new N_i and the LOS from this node allows N_t to be viewed and selected, completing the agent's route.

In addition, the flowchart for the node selection process and the movement of the agent in the AP-Theta* algorithm is shown in Fig. 7, where N_i = initial node; N_f = final node; N_t = target node; θ_x = angle of LOS; *Ma* = array of agents; *Px* = agent; e_x = edge of angle θ_x; x = value {1,2}; i = value {1…n}; d = distance: t = time; *Sn* = importance index.

The ORCA collision avoidance technique is also included in the algorithm. This is a low-dimensional linear program for collision-free movement.[21] It allows the early detection of possible collisions between multiple agents and static obstacles (furniture, walls, etc.) or dynamic obstacles (other agents in movement). Agent P located in the initial node N_i moves towards the target node N_t following a direct line of distance d between them. P moves at speed V and has

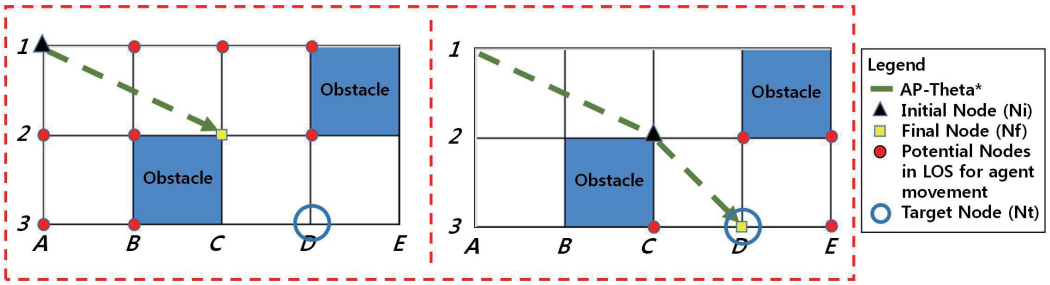

Fig. 6. (Color online) Displacement route using AP-Theta* pathfinding algorithm: (a) from N_{i1} [A1] to N_{f1} [C2], (b) from N_{i2} [C2] to N_t [D3].

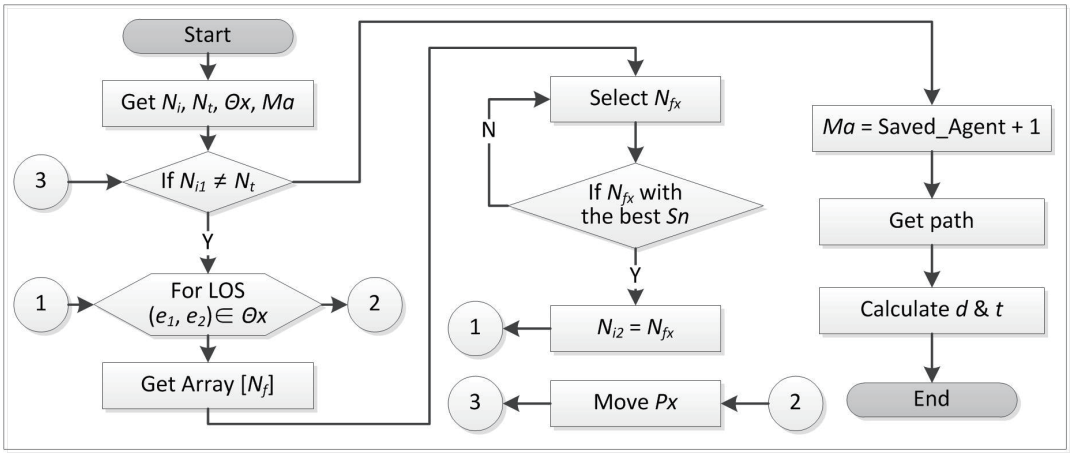

Fig. 7. Flowchart of the AP-Theta* pathfinding algorithm.

field of sight *fs* defined by angle θ. The route between N_i and N_t has two zones, the safe zone (*SZ*) and the risk zone (*RZ*). *RZ* is expanded as a buffer with a radius equal to 50% of *d* and its vertex varies with the location of *P*. The remaining area is classified as *SZ*. Static obstacles and dynamic agents are outside and inside *fs*. When the ORCA technique detects another agent as a possible obstacle located in *RZ* of *P*, *V* of both agents is modified equally, avoiding the collision. Because the agents evacuate towards the same N_t, simulations with a greater number of agents produce congestion in the selected routes. For this reason, an angle of minimum deviation β has been added to this technique. The size of β is set according to the number of agents around *RZ* and the width of the evacuation route. The operational flowchart of the ORCA collision avoidance technique is shown in Fig. 8, where N_i = initial node; N_t = target node; θ = angle of *fs*; *Mt* = array of path; *Px* = agent; *fs* = field of sight; *SZ* = safe zone; *RZ* = risk zone; *i* = value {1…*n*}; *d* = distance: *t* = time; *V* = speed.

The variable *v*0 maintains *Sn* of the vulnerability levels for every geometric element, thus influencing the movement of agents from N_i to N_t. The other conditioning variables included in the AP-Theta*-MVA algorithm are described below.

- The location of the hazard (*v*1) defines the starting position of the hazard, which is crucial for the algorithm to find alternative routes to the farthest exits from that location. We thus assume that children's facilities have more than one exit to the outside area. Each exit is assigned as a possible N_t for the multi-agent movement.
- The number of people (*v*2) defines the number of agents within a children's facility. Each person located in the facility is given the role of an agent, regardless of whether they are children, teachers, academic staff, or administrative staff. The simulation can be performed with a minimum of two agents. However, the number of agents is calculated on the basis of the maximum capacity of each of the spaces in the children's facility. The baseline is that the minimum space occupied by one person is 40 cm × 40 cm.[28]

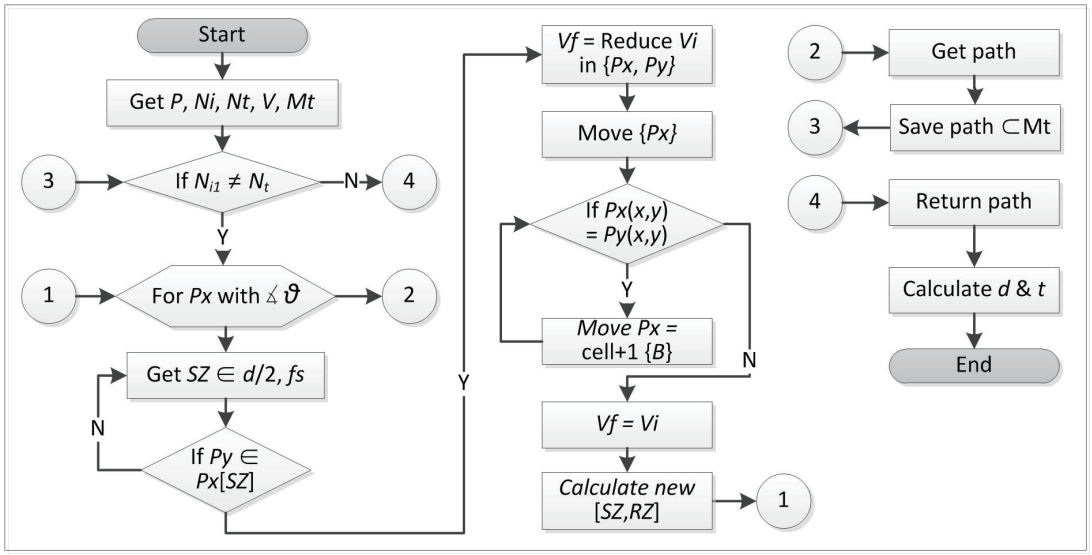

Fig. 8. Flowchart of ORCA collision avoidance.

- The speed of movement ($v3$) is the speed assigned for the movement of the group of agents. An important factor is that the main selected speed is 1.29 m/s, which represents the average movement of children in normal conditions.[29,30] This speed can vary in a close range according to the response of the ORCA, but the speed of 0 m/s is excluded because the simulation requires that the agents try to reach N_t.
- The reaction ability ($v4$) is defined as the aptitude of the agents to react and find the appropriate route to N_t when the simulation is started. Reaction ability is based on the foundations of Freud, who argues that people organized in crowds act differently from people as individuals;[31] each person in a crowd follows the behavior of the crowd and is less aware of their individual instincts. In addition, Stollard and Johnston described human movement as a physical science, where during an emergency situation, people exhibit irrational behavior and have different levels of panic.[32] For this reason, the modes and times of their reaction in their attempt to reach the exit are also different. In the assignment of the agents' reaction ability, the AP-Theta*-MVA algorithm interprets cases that the agents encounter. The cases are mutually exclusive and are shown graphically in Fig. 9. The first case is the reaction of a disoriented agent when approaching, within a defined radius, the exit door of a room or the intersection of corridors. The second case is that, within a defined radius of proximity to the disoriented agent, other agents that have already reacted and are following the same direction and movement pattern are detected. If the agent encounters either of these two cases, they receive instructions through signals that indicate the direction in which to proceed and link it to possible networks to move to N_t. In the AP-Theta*-MVA algorithm, a percentage value is also defined as an initial condition that represents the number of agents chosen at random who receive instructions for movement and have the ability to react when the simulation starts.

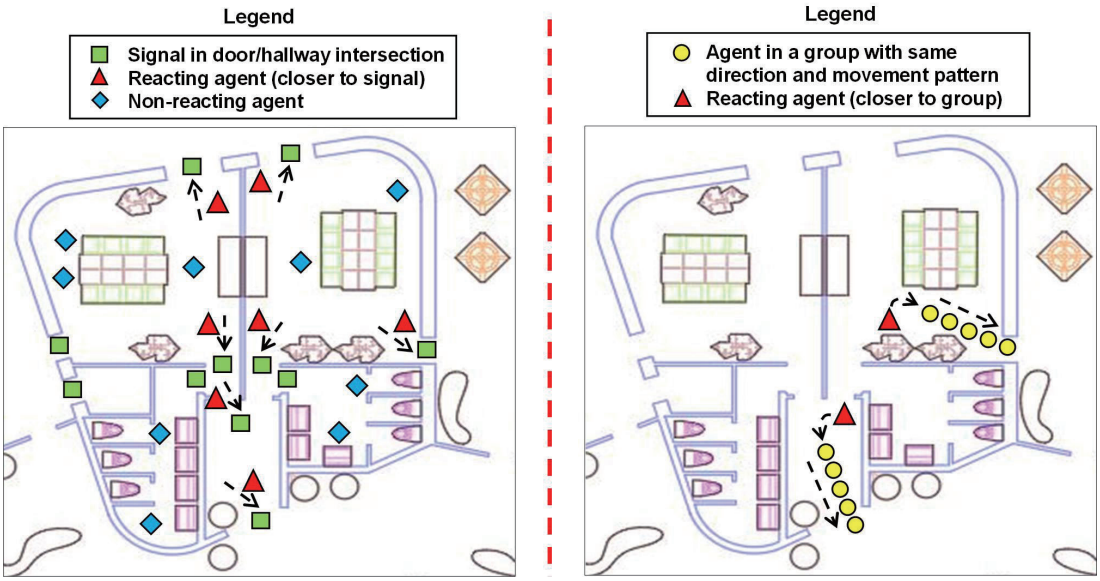

(a) (b)

Fig. 9. (Color online) Cases of assignment of agents' reaction ability: (a) location close to doors or hallway intersections and (b) in proximity to agents with same direction and movement pattern.

The simulations are divided into different scenarios, each of which is performed multiple times to enable a comparison of the results. Feasible multi-agent evacuation routes are obtained. The average evacuation time for the last agent to reach the target node is also calculated.

3. Experimental Results

To apply the methodology in children's facilities, a kindergarten of approximately 1320 m^2 with a complex nonlinear structure with many divisions is designed, as shown in Fig. 10. The structural elements included as part of the kindergarten are the walls, columns, divisions of classrooms, offices, and playgrounds. Doors are also included but under the assumption that they do not block the movement of the agents. Likewise, non-structural elements are included, such as fixed furniture, tables, chairs, armchairs, desks, playground games, computers, and breaker boxes. In addition, three exit doors are included in the design, denoted as E_x, where $x = \{1…3\}$. Exit E_1 is located in the lower left of the map, while exits E_2 and E_3 are located in the lower central and lower right areas, respectively.

The simplified geometric data is stored in a spatial database and is linked to the proposed vulnerability conditions based on international standards. On the basis of the standards of Technical Assistance for People with Disabilities of the ADA,[25] we consider vulnerability condition ct_1, which is related to the width and dimensions of interior spaces. This is a very important factor in a multi-agent system since it influences the sequential or parallel evacuation of agents, as well as the possibility that the collision avoidance technique has a greater range to widen the angle of deviation in crowded situations. The other vulnerability conditions selected in the research are the construction site condition ct_2, the architectural configuration ct_3, the architectural partitions ct_4, the structural systems ct_5, the building envelope ct_6, and the mechanical conditions ct_7. All of them belong to the standards of the Design Guide for Improving

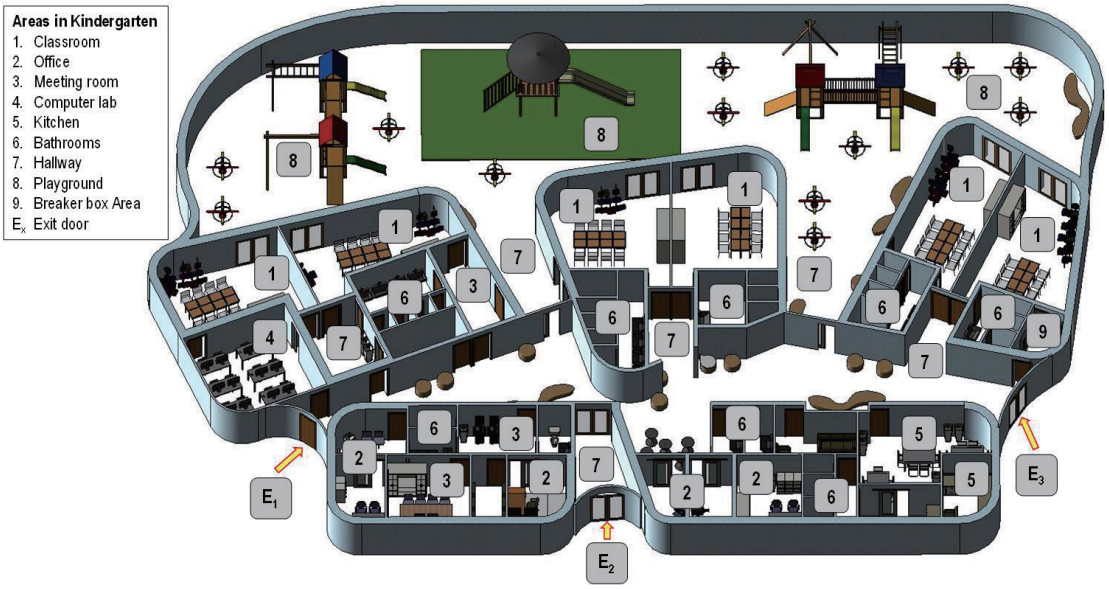

Fig. 10. (Color online) Distribution of areas in kindergarten.

School Safety in Earthquakes, Floods, and High Winds, proposed by FEMA of the United States.[2] Table 3 shows in detail the suitability model for this study, in which the different types of vulnerability have been classified according to their response to the occurrence of smoke spreading from a fire. For the classification of the multilayers of vulnerability, five levels of suitability are assigned. A value of 1 represents the most suitable condition for the movement of the multi-agent system, because the vulnerability of the geometric element is very low. On the other hand, a value of 5 represents the least suitable condition for movement, since the vulnerability is very high.

Subsequently, the paired comparison matrix proposed by Saaty[19] is used and the levels of influence between these vulnerability conditions are obtained. These weights are set to achieve the objective of the simulations, which is to calculate safe evacuation routes within children's facilities. In addition, the consistency between these comparisons is analyzed. Table 4 shows the

Table 3
Suitability model for vulnerability.

ID & Vulnerability	Classification of vulnerability levels and suitability				
	Highly suitable (1)	Suitable (2)	Moderately suitable (3)	Unsuitable (4)	Highly unsuitable (5)
ct_1 Width and dimensions	>2285 mm	2285 mm	< 2285 mm & > 915 mm	915 mm	< 915 mm
ct_2 Site condition	Two or more means of site access	Two means of site access	Structure elevated on fill	In medium proximity to high-risk facilities for hazards	In close proximity to high-risk facilities for hazards
ct_3 Architectural configuration	Regular building forms	—	Enclosed courtyard building forms	Large roof overhangs. Re-entrant corner building forms	Very complex building forms
ct_4 Architectural partitions	Concrete block, hollow clay tile around exit ways and stairs	Block, hollow clay tile partitions. Parapet	Heavy roof	Non-rigid connections for attaching interior non-load bearing walls to structure	Gypsum wallboard partitions
ct_5 Structural systems	Concrete or reinforced masonry (CMU) exterior structural walls	Heavy structure: reinforced concrete (RC) masonry, RC or masonry fireproofing of steel	Ductile detailing and connections/ steel. Design for uplift (wind). Ductile detailing/ RC	Light structure: steel/wood. Seismic separation joints	Unreinforced masonry (URM) exterior load bearing walls. Soft/weak first floor. Indirect load path. Discontinuities in vertical structure
ct_6 Building envelope	Contains no wall cladding or glazing	Contains simple or decorative wallcoverings	Masonry veneer on exterior walls	Impact-resistant glazing	Metal/glass curtain wall
ct_7 Mechanical conditions	—	Heating, ventilation, and air conditioning system designed for purging	—	Large rooftop-mounted equipment	—

Table 4
Paired comparison matrix.

	Matrix ***A*** = Paired Comparison Matrix							Matrix ***B*** = Normalized Comparison Matrix							(*w*)	A_{max}	*CI*	*CR*
	ct_1	ct_2	ct_3	ct_4	ct_5	ct_6	ct_7	ct_1	ct_2	ct_3	ct_4	ct_5	ct_6	ct_7				
ct_1	1	2	3	4	6	7	9	0.40	0.47	0.44	0.31	0.31	0.25	0.23	0.34	7.71	0.12	
ct_2	0.50	1	2	4	5	7	8	0.20	0.24	0.29	0.31	0.26	0.25	0.20	0.25	7.85	0.14	
ct_3	0.33	0.50	1	3	5	6	7	0.13	0.12	0.15	0.23	0.26	0.21	0.18	0.18	7.87	0.14	
ct_4	0.25	0.25	0.33	1	2	4	7	0.10	0.06	0.05	0.08	0.10	0.14	0.18	0.10	7.40	0.07	
ct_5	0.17	0.20	0.20	0.50	1	3	5	0.07	0.05	0.03	0.04	0.05	0.11	0.13	0.07	7.26	0.04	
ct_6	0.14	0.14	0.17	0.25	0.33	1	3	0.06	0.03	0.02	0.02	0.02	0.04	0.08	0.04	7.08	0.01	
ct_7	0.11	0.13	0.14	0.14	0.20	0.33	1	0.04	0.03	0.02	0.01	0.01	0.01	0.03	0.02	7.19	0.03	
∑	2.50	4.22	6.84	12.9	19.6	28.3	40.0								1.00	7.48	0.08	0.061

calculations of the paired matrix between the seven criteria. The weight *w* is the average of the values for each vulnerability condition of the normalized comparison matrix ***B***. Likewise, the eigenvector A_{max} is the result of multiplying matrix ***B*** and *w*. The consistency index *CI* is calculated as the average $(A_{max}-n)/(n-1)$, where *n* is the number of vulnerability conditions. After dividing *CI* by the random consistency index *RI*, the consistency ratio *CR* is obtained. Using *RI* = 1.32, *CR* for Table 4 is 6.1%, which is acceptable for ensuring the consistency between the conditions.[19]

After the rasterization of the vulnerability layers, the weight factors are assigned to each condition to obtain *Sn*. The graphical results are shown in Fig. 11. Likewise, in Fig. 12, the study area is shown in two vulnerability situations. Figure 12(a) shows vulnerability situation A (VSA), which uses the AP-Theta* algorithm and does not include the calculated *Sn*, showing all free areas as walkable without restrictions or levels of vulnerability. On the other hand, Fig. 12(b) shows vulnerability situation B (VSB) using the proposed AP-Theta*-MVA algorithm, which integrates and analyzes in a single layer the average of *Sn* for all the vulnerability conditions.

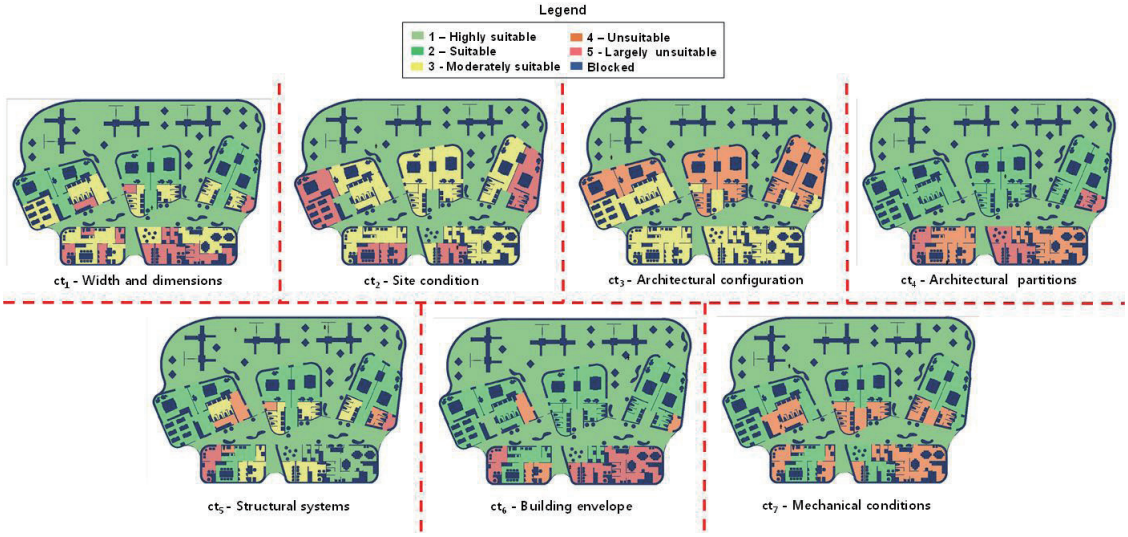

Fig. 11. (Color online) Weight factor values by vulnerability conditions.

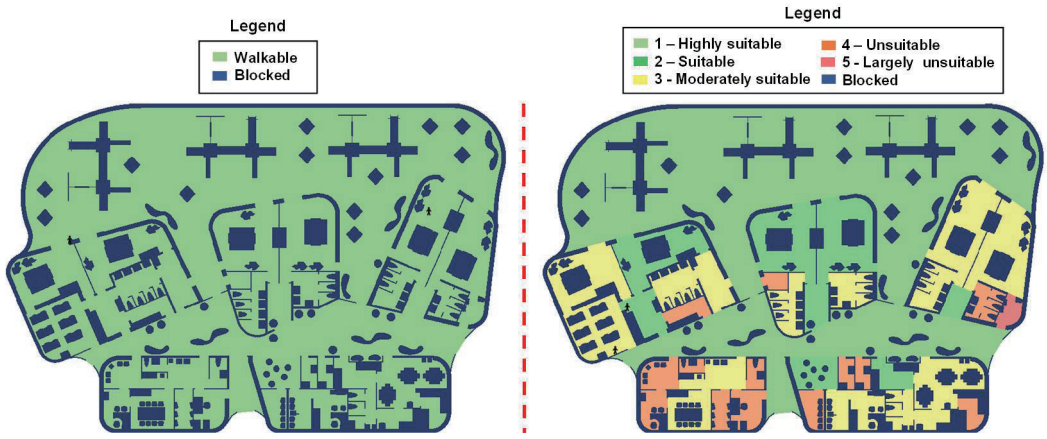

Fig. 12. (Color online) Vulnerability situations for simulations: (a) VSA without *Sn* and (b) VSB including *Sn*.

Simulations are conducted to calculate the evacuation routes and times of multi-agent systems for the kindergarten in the case study. The simulations are performed using the open software NetLogo. This software allows the modeling of different scenarios, with their initial conditions modified via the conditioning variables: the location of the hazard ($v1$), the number of people ($v2$), and their speed of movement ($v3$) and reaction capacity ($v4$). For the case study, different combinations of the conditioning variables are set in advance, which provide 16 simulation scenarios for VSA and VSB, as detailed in Table 5.

The location $v1$ is given two sub-conditions. In the first one, smoke spread by a fire starts in the playground away from the classrooms. In the second one, it starts in the breaker box room located next to exit door E_3, which is blocked and cannot be used as an evacuation route. The

Table 5
Conditioning variables for multi-agent simulation scenarios.

Simulation scenario	($v1$) Location of hazard	($v2$) Number of people	($v3$) Children's speed (m/s)	($v4$) Reaction ability (%)
VSA01 / VSB 01	Playground	105	1.3	25
VSA02 / VSB 02				50
VSA03 / VSB 03			2.6	25
VSA04 / VSB 04				50
VSA05 / VSB 05		210	1.3	25
VSA06 / VSB 06				50
VSA07 / VSB 07			2.6	25
VSA08 / VSB 08				50
VSA09 / VSB 09	Breaker box room	105	1.3	25
VSA10 / VSB 10				50
VSA11 / VSB 11			2.6	25
VSA12 / VSB 12				50
VSA13 / VSB 13		210	1.3	25
VSA14 / VSB 14				50
VSA15 / VSB 15			2.6	25
VSA16 / VSB 16				50

number of people $v2$ is also given two initial sub-conditions. In the first one, the normal capacity of 105 people located in classrooms, computer labs, offices, and meeting rooms is used. In the second sub-condition, there are 210 people, double the capacity, i.e., the facility is crowded. For the speed $v3$, the given sub-conditions are 1.3 m/s, which represents the average speed of children's movement, and 2.6 m/s, which is twice the average. For the reaction ability $v4$, the ability to react and move toward the target node is assigned to 25 or 50% of the agents chosen at random when the simulation starts. Because a kindergarten is considered, most people are expected to be children, who require more time than adults to understand the danger of a situation and perform the evacuation. The remaining agents without the ability to react or move towards the target node react later when they comply with any of the rules of the variable. The first configured rule is that the agent is located or approaches to less than 2 m away from a door or hallway intersection. The second rule is that the agent detects at least five other agents with the same movement pattern and direction within a radius of 2 m from their current location.

In addition to the initial conditions for simulating scenarios, rules are applied for the proper operation of AP-Theta*-MVA under the AP-Theta* pathfinding and ORCA collision avoidance machine learning techniques. The rules cover the conditions of movement of the agents, as well as the displacement of the smoke due to the fire. These rules are classified into general rules for AP-Theta*-MVA and specific rules for each technique.

General rules for simulations in the AP-Theta*-MVA algorithm:

- All grid cells are homogeneous and isotropic.
- People are added as dynamic agents in the model.
- Each cell has a 'free' or 'blocked' condition for the movement of the agent and the hazard.
- There are three cells marked as N_t located in exit doors E_1, E_2, and E_3 of the facility.
- Free cells contain a marker that stores their Sn.
- The agents move on the basis of signals set as conditions of the reaction ability variable.
- The velocity of movement of the agents is set by the speed variable.
- The smoke spreads from its initial location to the surrounding free cells under the MG method.
- If the smoke reaches a free cell, it is marked as 'dangerous free' and its color is changed to red.
- When an agent reaches N_t, the 'saved people' counter increases by one unit.
- If an agent cannot move to a free cell and the smoke reaches the agent, the agent stops, turns light blue, and the 'trapped people' counter increases by one unit.
- The model ends when all agents reach the available N_t or are trapped by the smoke, i.e., no more agents are moving in the kindergarten.
- For each simulation, the model execution time is calculated and stored together with the numbers of saved people and trapped people.

Rules related to AP-Theta* pathfinding technique:

- The agents attempt to reach the closest N_t along their LOS from their N_i.
- Agents can only move through cells with a value of Sn greater than or equal to that at their current location.
- Agents cannot move through cells marked 'blocked'.

Rules related to the ORCA collision avoidance technique:

- Two or more agents cannot occupy a cell at the same moment of the simulation.
- Agents cannot move through 'dangerous free' cells or through 'blocked' cells.
- If two agents are on a collision course, they both reduce their speed equally and the deviation angle is applied.
- If a 'dangerous free' cell or 'blocked' cell is in the way of an agent, then the agent changes their route to avoid it.

Simulations are performed through NetLogo for the 16 multi-agent systems in the VSA scenarios using the AP-Theta* algorithm, which does not consider *Sn*, and for the other 16 multi-agent systems in the VSB scenarios using the AP-Theta*-MVA algorithm, which considers *Sn*. Each simulation scenario is executed 100 times to obtain the average evacuation time and number of saved agents. The number of saved agents is converted to a percentage because the total number of agents fluctuates as defined in Table 5. The average evacuation time, percentage of saved agents for each simulation scenario, and the evacuation time difference between VSB and VSA are shown in Table 6.

From the results of Table 6, it is clear that the VSA and VSB simulation scenarios for groups 01 to 08 have shorter evacuation times than those for groups 09 to 16. This is because in the former, the smoke starts in the playground, located on the opposite side of the exit doors, which forces the agents to escape through the most direct routes. However, in the latter, the hazard starts near exit door E_3, forcing the agents to search for alternative routes to the shortest path or the safest path according to their *Sn*. The difference in evacuation times between the VSA simulation scenarios (for which the shortest routes are searched for) and VSB scenarios (for which the safest routes are searched for) fluctuates between 1.5 and 2.5 s for groups 01 to 08 and

Table 6
Average evacuation time and number of saved agents for each multi-agent simulation scenario.

VSA scenario	(A) Average evacuation time (s)	Saved agents (%)	VSB scenarios	(B) Average evacuation time (s)	Saved agents (%)	(B) – (A) Evacuation time difference (s)
VSA01	16.3	99.5	VSB 01	17.9	98.6	1.6
VSA02	15.4	99.5	VSB 02	16.9	99.0	1.5
VSA03	9.5	99.0	VSB 03	12.0	98.6	2.5
VSA04	7.8	99.5	VSB 04	10.1	99.0	2.3
VSA05	21.2	98.1	VSB 05	23.3	97.1	2.2
VSA06	19.9	98.6	VSB 06	22.2	98.1	2.3
VSA07	13.4	99.0	VSB 07	15.3	98.6	1.9
VSA08	11.1	99.5	VSB 08	12.8	99.0	1.7
VSA09	18.3	95.2	VSB 09	21.4	90.1	3.1
VSA10	17.2	96.7	VSB 10	20.8	92.4	3.6
VSA11	12.9	99.0	VSB 11	16.3	97.1	3.4
VSA12	10.7	99.5	VSB 12	14.1	98.1	3.4
VSA13	23.8	89.0	VSB 13	27.1	87.1	3.3
VSA14	21.6	91.4	VSB 14	25.4	88.6	3.8
VSA15	16.4	97.6	VSB 15	19.9	95.7	3.5
VSA16	13.8	99.0	VSB 16	16.7	97.6	2.9

between 2.9 and 3.6 s for groups 09 to 16. According to the analysis of the evacuation routes, the results for the VSB simulation scenarios are highly influenced by the vulnerability conditions of their *Sn*. The safest routes calculated for agent movement will be much longer than the direct routes traced in the VSA simulation scenarios, where vulnerability is not considered. Specifically, two cases (VSA06/VSB06 and VSA14/VSB14) are shown as examples, where the movement behavior of the agents and the routes they follow in different simulation scenarios are analyzed.

Figure 13(a) graphically shows VSA06 after 5, 10, and 20 s, while Fig. 13(b) shows VSB06 after the same times. Both scenarios have the same variables: the initial location of the hazard is in the playground, 210 people are in the classrooms and offices of the kindergarten, the children's movement speed is 1.3 m/s, and their reaction ability is 50%. By analyzing these groups of images, the direction pattern and evacuation routes chosen by the agents on their way to some of the target nodes are traced. In the VSA06 scenario, since *Sn* are not considered, the agents take the shortest routes, which cross vulnerable areas such as computer labs, classrooms, and offices. However, in the VSB06 scenario, routes through corridors and passageways are prioritized, because *Sn* of these areas have low vulnerability values.

Figures 14(a) and 14(b) show VSA14 and VSB14 after 5, 10, and 20 s, respectively. In both cases, the initial location of the hazard is in the breaker box room, very close to exit door E_3, which is blocked after the event starts. For this reason, in this scenario, the agents move towards exit doors E_1 and E_2, which are the remaining escape alternatives. In VSA14 and VSB14, the

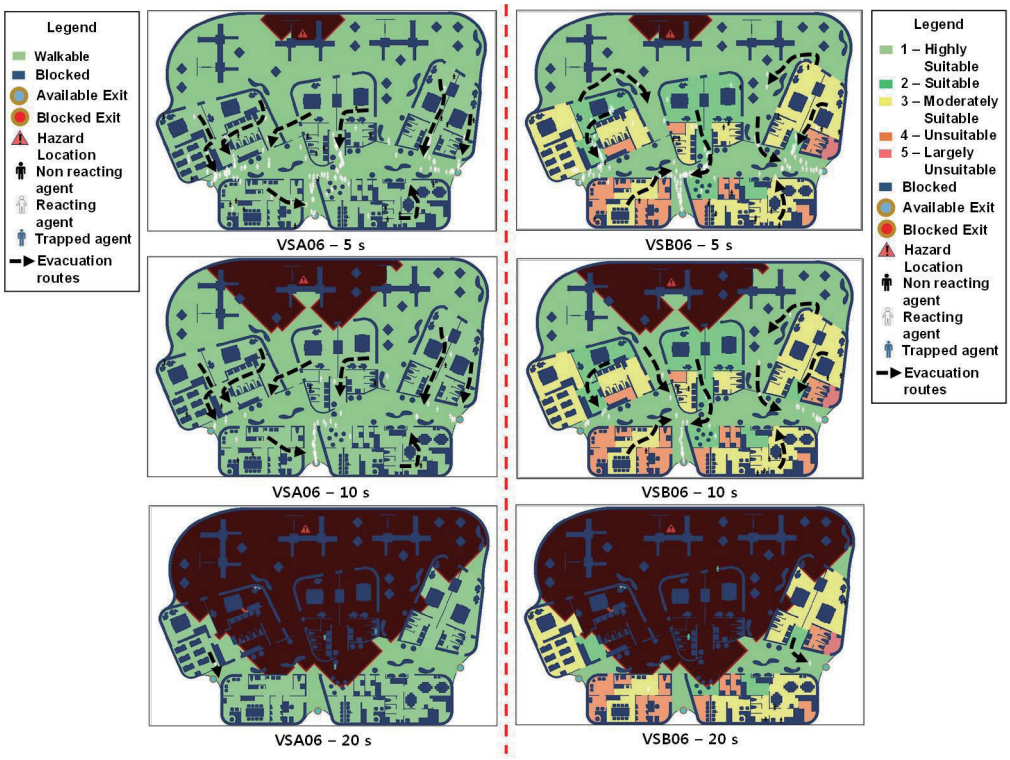

(a) (b)

Fig. 13. (Color online) Multi-agent simulation scenarios (a) VSA06 and (b) VSB06.

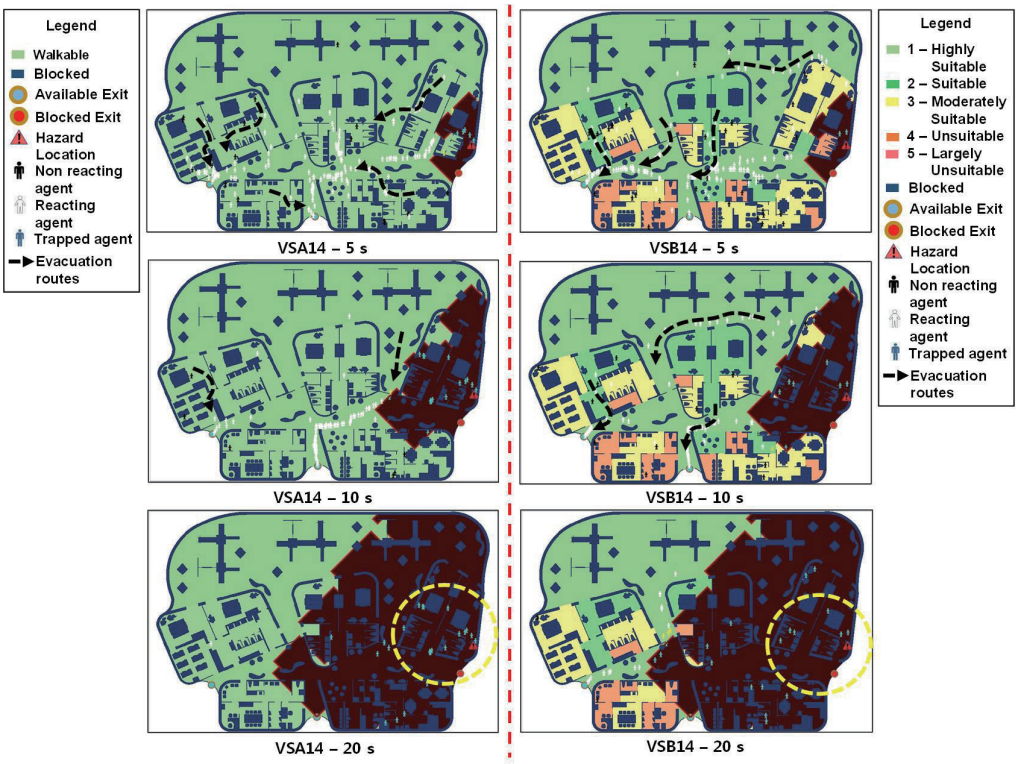

Fig. 14. (Color online) Multi-agent simulation scenarios (a) VSA14 and (b) VSB14.

behavior and movement pattern of the agents are very similar to those in the previous example. For VSA14, the agents are able to cross vulnerable areas and trace shorter paths, but in VSB14, the agents move through the safer zones.

One of the main advantages of applying *Sn* is shown at time 20 s in Fig. 14, in which the area surrounding the initial location of the hazard has been marked with a yellow circle. In the case of VSA14, because the agents look for the shortest route to escape, many of them approach the area where the smoke has spread, becoming trapped. In this situation, smoke becomes a dangerous obstacle on the shortest route selected by agents that do not consider *Sn*. However, in the case of VSB14, the agents move through less vulnerable areas, resulting in a small number of agents trapped near the place where the hazard started. This issue is fundamental and often arises in the simulation scenarios where the location of the hazard is close to exit door E_3. Therefore, in the VSB scenarios, the smoke represents an obstacle that the agents try to avoid when considering *Sn*.

The analysis of the results allows us to validate the influence of the MVA and the conditioning variables in the processing of the AP-Theta*-MVA algorithm. In addition, the algorithm is efficient when calculating evacuation route patterns under the rules of the AP-Theta* pathfinding and ORCA collision avoidance machine learning techniques. With the AP-Theta* rules, evacuation routes are calculated according to the agent's LOS to the target node. With the ORCA rules, these routes are slightly offset to avoid collisions when agents move towards the same

node. Likewise, AP-Theta*-MVA mainly commands agents to move towards the target node based on signals when they have reaction ability. The difference in evacuation times between the VSA and VSB simulation scenarios in a multi-agent environment is less than 3.7 s for a children's facility with an area of 1320 m^2. Furthermore, as shown in Table 6, the percentages of agents evacuated in the VSA and VSB vulnerability situations are above 89 and 87.1%, respectively. However, we must consider that the initial conditions of the location of the hazard, the number of people, and their speed and reaction ability differ for each scenario, as indicated in Table 5.

The proposed algorithm has the ability to calculate safer evacuation routes that are longer than the shortest routes but ensure a higher probability that more people escape. Specifically, for the VSB simulation scenarios, the routes are traced on the basis of the influence of their *Sn*, which classify the vulnerability levels of different areas of the kindergarten. These results are essential for decision makers to evaluate the safety of evacuation routes in areas with highly vulnerable people such as children. The criteria applied by the proposed algorithm should be considered within the evacuation plans and safety standards of governments both when designing children's facilities and when signaling more effective escape routes in existing facilities.

4. Conclusions

In this paper, we proposed the calculation of safer evacuation routes within children's facilities through the use of the AP-Theta*-MVA algorithm, which combines AP-Theta* pathfinding and ORCA collision avoidance machine learning techniques. The algorithm includes importance indexes (*Sn*), which are obtained by applying MVA to the objects within children's facilities. These indexes are spatially distributed in the geometric elements of the facilities. The algorithm also includes conditioning variables such as the location of the hazard, the number of people, their speed of movement, and their reaction ability, which were varied in this study to create different simulation scenarios. The methodological processing is divided into three stages. In the first stage, the data of the children's facilities is prepared in a BIM following IFC standards and is transformed into geometric elements for storage in a spatial database. In the second stage, the MVA is carried out using a suitability matrix based on international standards to calculate *Sn* for the simplified geometry. Then, using the AHP, the consistency of the vulnerability data in the installations is guaranteed. In the third stage, using the AP-Theta*-MVA algorithm, feasible evacuation patterns and routes are obtained for various simulation scenarios.

In our simulations, we applied the algorithm to the case of evacuation from a children's facility and calculated the evacuation patterns and routes of the multi-agent system. We compared evacuation times for different scenarios based on two vulnerability situations: VSA, in which the AP-Theta* algorithm was used, which did not include *Sn* of the vulnerability of different locations in the facility place, and VSB, in which the new AP-Theta*-MVA algorithm was used, which includes the results of *Sn*. For each vulnerability situation, 16 simulation scenarios with different combinations of conditioning variables were considered. This allowed us to perform a better analysis of the results by comparing the multi-agent situation under various evacuation conditions.

The experimental results revealed that performing the MVA on the geometric elements has a strong influence on the VSB results when the AP-Theta*-MVA algorithm chooses the evacuation routes while prioritizing areas of less vulnerability. Comparing these results with those obtained from VSA using the AP-Theta* algorithm, a small increase in the evacuation time and a slight decrease in the percentage of evacuated agents were observed. These differences observed in the simulations are expected to be key factors for decision makers and planners in design and construction. When they propose evacuation routes, they must assess the feasibility of using safer routes that prioritize low-vulnerability areas versus shorter routes that prioritize time, especially in facilities with highly vulnerable people such as children.

Acknowledgments

This research was supported by a grant (2021R1F1A106422811) from the Basic Research Project for Science and Engineering funded by the Ministry of Science and ICT of the Korean government.

References

1 P. J. Landrigan: Hum. Ecol. Risk Assess. **11** (2006) 235. https://doi.org/10.1080/10807030590920051
2 Federal Emergency Management Agency FEMA: https://www.fema.gov/sites/default/files/documents/fema_p-424-design-guide-improving-school-safety.pdf (accessed February 2022).
3 Department of Education and Children's Services of the Government of South Australia: https://www.education.sa.gov.au/sites/default/files/early-childhood-facilities-birth-to-age-8-design-standards-and-guidelines.pdf?v=1459296603 (accessed February 2022).
4 U.S. Department of Defense: https://www.wbdg.org/FFC/DOD/UFC/ufc_4_740_14_2002.pdf (accessed February 2022).
5 U.S. General Service Administration: https://www.gsa.gov/cdnstatic/designguidesmall.pdf (accessed February 2022).
6 Z. Xu and M. Doren: IEEE Int. Conf. Comput. Sci. Autom. Eng. **1** (2011) 62. https://doi.org/10.1109/CSAE.2011.5953171
7 N. Weerasekara: Master's Thesis, Illinois State University (Illinois, USA, 2015) 67. https://ir.library.illinoisstate.edu/etd/389 (accessed February 2022).
8 S. H. Yoo, M. K. Kim, J. S. Bae, and H. G. Sohn: J. Korean Soc. Surv. Geod. Photogramm. Cartog. **36** (2018) 573. https://doi.org/10.7848/ksgpc.2018.36.6.573
9 E. W. Dijkstra: Numer. Math. **1** (1959) 269. https://doi.org/10.1007/BF01386390
10 P. Hart, N. Nilsson, and B. Raphael: IEEE Trans. Syst. Sci. Cybern. **4** (1968) 100. https://doi.org/10.1109/TSSC.1968.300136
11 K. Daniel, A. Nash, S. Koenig, and A. Felner: J. Artif. Intell. Res. **39** (2010) 533. https://doi.org/10.1007/BF01386390
12 A. Naderpour: Master's Thesis, University of Washington (Washington, USA, 2018) 92. http://hdl.handle.net/1773/41704 (accessed February 2022).
13 D. Helbing, I. Farkas, and T. Vicsek: Lett. Nat. **407** (2000) 487. https://doi.org/10.1038/35035023
14 Q. Huang, H. Ma, and H. Zang: IEEE Int. Conf. Rob. Intell. Syst. Signal Process. **2** (2003) 1036. https://doi.org/10.1109/RISSP.2003.1285732
15 M. Moussaid, D. Helbing, and G. Theraulaz: Proc. Natl. Acad. Sci. **17** (2011) 6884. https://doi.org/10.1073/pnas.1016507108
16 M. Chennoufi, F. Bendella, and M. Bouzid: Int. J. Ambient Comput. Intell. **9** (2019) 43. https://doi.org/10.4018/IJACI.2018010103
17 E. E. Castillo Osorio and H. H. Yoo: J. Korean Soc. Surv. Geod. Photogramm. Cartog. **37** (2019) 303. https://doi.org/10.7848/ksgpc.2019.37.5.303
18 T. L. Saaty: J. Math. Psychol. **15** (1977) 234. https://doi.org/10.1016/0022-2496(77)90033-5

19 T. L. Saaty: Eur. J. Oper. Res. **48** (1990) 9. https://doi.org/10.1016/0377-2217(90)90057-I
20 E. E. Castillo Osorio, M. S. Seo, and H. H. Yoo: Sens. Mater. **32** (2020) 3835. https://doi.org/10.18494/SAM.2020.2908
21 J. van de Berg, S. J. Guy, M. Lin, and D. Manocha: Rob. Res. **70** (2011) 3. https://doi.org/10.1007/978-3-642-19457-3_1
22 I. Hong and A. T. Murray: Trans. GIS. **20** (2016) 570. https://doi.org/10.1111/tgis.12160
23 X. Li, I. Hijazi, M. Zu, H. Lv, and R. El Meouche: Multimedia Tools Appl. **75** (2016) 17449. https://doi.org/10.1007/s11042-015-3156-6
24 U. Isikdag, S. Zlatanova, and J. Underwood: Comput. Environ. Urban Syst. **41** (2013) 112. https://doi.org/10.1016/j.compenvurbsys.2013.05.001
25 U.S. Department of Justice Civil Rights Division: https://www.ada.gov/2010ADAstandards_index.htm (accessed February 2022).
26 R. W. Saaty: Math. Modell. **9** (1987) 161. https://doi.org/10.1016/0270-0255(87)90473-8
27 E. E. Castillo Osorio, M. S. Seo, and H. H. Yoo: J. Korean Soc. Surv. Geod. Photogramm. Cartog. **39** (2021) 265. https://doi.org/10.7848/ksgpc.2021.39.5.265
28 U. Weidmann: Transporttechnik der Fussganger - Transporttechnische Eigenschaften des Fussgangerverkehrs, Literaturauswertung (1992) (in German). https://doi.org/10.3929/ethz-a-000687810
29 A. T. K. Pinheiro, A. Hokugo, and T. Nishino: J. Archit. Plann. **79** (2014) 583. https://doi.org/10.3130/aija.79.583
30 L. Carcreff, C. N. Gerber, A. Paraschiv - Ionescu, G. De Coulon, K. Aminian, C. J. Newman, and S. Armand: J. Front. Bioeng. Biotechnol. **8** (2020) 812. https://doi.org/10.3389/fbioe.2020.00812
31 S. Freud: Group Psychology and the Analysis of the Ego, The Standard Edition of the Complete Psychological Works of Sigmund Freud, Volume XVIII (1920–1922): Beyond the Pleasure Principle, Group Psychology and Other Works, p. 65.
32 P. Stollard and L. Johnston: Design against Fire: An Introduction to Fire Safety Engineering Design, Spons Architecture Price Book (London, England, 1994) 1st ed., p. 172.

About the Authors

Ever Enrique Castillo Osorio received his B.S. degree from Inca Garcilaso de la Vega University, Peru, in 1999 and his M.S. degree from Gyeongsang National University, Republic of Korea, in 2017. He is currently working on his Ph.D. degree. From 2000 to 2015, he worked in ICT and GIS at the Meteorology and Hydrology Service of Peru. His research interests include GeoAI and disaster risk management. (ever.castillo.osorio@gmail.com)

Min Song Seo received her B.S. and M.S. degrees from Gyeongsang National University, Republic of Korea, in 2016 and 2018, respectively. She is currently working on her Ph.D. degree. Her research interests are in GIS analysis using big data. (msong7938@gmail.com)

Hwan Hee Yoo received his B.S. degree from Kangwon National University, Republic of Korea, in 1981 and his M.S. and Ph.D. degrees from Yonsei University, Republic of Korea, in 1983 and 1988, respectively. Since 1990, he has been a professor at Gyeongsang National University, Korea. He served as the president of Korean Society for Geospatial Information Science from 2009 to 2010. His research interests are in GIS and big data analysis. (hhyoo@gnu.ac.kr)